Yield of K X Rays Emitted from U^{236} Fragments

S. S. KAPOOR, V. S. RAMAMURTHY, AND R. ZAGHLOUL*

Bhabha Atomic Research Centre, Trombay, India

(Received 6 August 1968)

The yield of K x rays from different fragment masses have been determined in the thermal-neutron-induced fission of U^{235}. The energies of the pairs of fragments were measured with two semiconductor detectors placed on either side of a thin U^{235} foil. The K x rays from the light and the heavy groups of fragments were separated by measuring the x-ray energies with a 1-mm NaI(Tl) crystal. The fragment mass distributions in coincidence with the light group of K x rays and with the heavy group of K x rays, and the unbiased mass distributions, were simultaneously recorded in different quarters of a 1024-channel analyzer memory. From these distributions, after suitable corrections for the background, x-rays detection efficiencies, and finite-energy-resolution effects, the number of x rays as a function of fragment mass has been determined. The x-ray yield per fission is found to be 0.08±0.01 for the light fragment group, and 0.30±0.02 for the heavy fragment group. The gross features of the yield as a function of mass are similar to those observed earlier for emission from Cf^{252} fragments. However, unlike the case of Cf^{252}, for masses greater than 144 the striking increase in the yield is not observed. The present results are consistent with the interpretation that the x-ray yield depends both on the characteristics of the low-lying states and the initial spin of the fragments.

I. INTRODUCTION

PREVIOUS investigations[1-4] have shown that almost all the K x rays emitted in fission result from the internal conversion process during the γ de-excitation of the fragments. Consequently, it is now realized that a measurement of the number of K x rays emitted from individual fragments can provide useful information about the internal conversion probabilities in the emitting fragment and thereby about the relative abundance of the low-energy transitions in these neutron-rich nuclei. So far such extensive studies of the K x-ray emission have not been carried out for the case of thermal neutron fission of various fissile nuclei and whatever results are available,[5-9] the agreement between them is poor. In the present work, the emission of K x rays in the thermal neutron fission of U^{235} have been studied to determine the K x ray yield as a function of fragment mass.

II. EXPERIMENTAL

A. Apparatus

A schematic diagram of the experimental arrangement is shown in Fig. 1. A source of U^{235} of thickness 250 $\mu g/cm^2$ coated on an area of 0.5 cm² of a thin VYNS film by the electrospraying technique was used in the measurements. The kinetic energies of the pairs of fragments were measured by two diffused junction silicon detectors placed on either side of the source foil at distances of 2.2 and 1.6 cm, all mounted inside an evacuated chamber. The x-ray energies were measured with a 1 mm NaI(Tl) crystal of 9 cm² area covered with a 0.008-in. beryllium window and mounted on a 6292 photomultiplier tube. As shown in Fig. 1, the x-ray detector was carefully shielded from the direct beam and was placed at right angles to the line joining the fission detectors. A collimated neutron beam from a beam hole of the CIRUS reactor served as the neutron source. To reduce the γ-ray flux, the beam from the reactor core passed through 10 in. of bismuth and finally through a steel collimator that reduced the beam diam to $\frac{1}{2}$ in. The neutron beam was made to enter the fission

* On leave from U.A.R. Atomic Energy Establishment, Cairo. Present address: Reactor Physics Group, A.E.E., Cairo, U.A.R.
[1] L. E. Glendenin and H. C. Griffin, Phys. Letters 15, 153 (1965). L. E. Glendenin and J. P. Unik, Phys. Rev. 140, B1301 (1965).
[2] S. S. Kapoor, H. R. Bowman, and S. G. Thompson, Phys. Rev. 140, B1310 (1965).
[3] R. A. Atneoson, T. D. Thomas, W. H. Gibson, and M. L. Perlman, Phys. Rev. 148, 1206 (1966).
[4] R. L. Watson, H. R. Bowman, and S. G. Thompson, Phys. Rev. 162, 1169 (1967).
[5] V. V. Sklyarevskii, E. P. Stepanov, and B. A. Medvedev Zh. Eksperim. i Teor. Fiz. 36, 326 (1959) [English transl.: Soviet Phys.—JETP 9, 225 (1959)].
[6] H. Hohman, Z. Physik 172, 143 (1963).
[7] L. Bridwell, M. E. Wyman, and B. W. Wehring, Phys. Rev. 145, 963 (1966).
[8] B. W. Wehring and M. E. Wyman, Phys. Rev. 157, 1083 (1967).
[9] V. P. Eismont and V. A. Yurgenson, Yadern Fiz. 5, 1192 (1967) [English transl.: Soviet J. Nucl. Phys. 5, 852 (1967)].
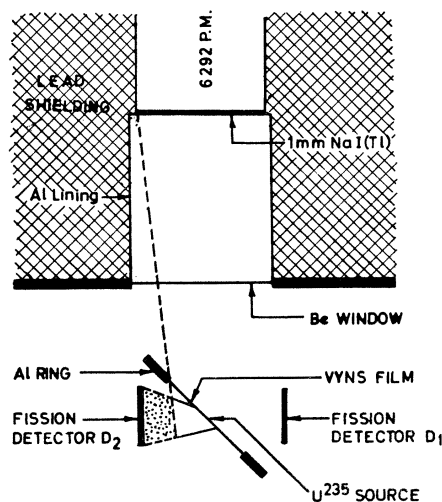

FIG. 1. Schematic diagram of the experimental arrangement for determining the K x-ray yield from different fragments.

FIG. 2. Block diagram of the electronic arrangement for K x-ray yield determination.

chamber through two aluminized Mylar windows to avoid scattering of the beam at the chamber walls. The U^{235} foil was mounted on a rod fixed at an angle of 45° to the top plate of the chamber in such a way that the foil was at an angle of 45° each to the incident beam, the line joining the fission detectors and the line joining the center of the foil and the x-ray detector. The x rays were detected through a 0.01 in. beryllium window of 1.25 in. diam fixed at the center of the base plate of the chamber. In this geometry the distance of the NaI(Tl) crystal from the center of the foil was fixed at 3.2 in. (8.1 cm).

B. Procedure and Electronics

The method consisted in simultaneously measuring the fragment mass distributions in coincidence with the light group of K x rays, heavy group of K x rays and without regard to any secondary radiations. From these distributions, after correction for the background, x-ray detection efficiencies, and the finite energy-resolution effects, the K x-ray yield as a function of fragment mass were obtained. Figure 2 shows the block diagram of the electronic arrangement. The pulse-height distributions from the fission detectors D_1 and D_2 were first matched by adjusting the amplifier gains. The amplified pulse heights V_1 and V_2 from detectors D_1 and D_2, respectively, were then fed to an adder-divider circuit that generated a pulse proportional to $V_2/(V_1+V_2)$. As also pointed out by Atneoson et al.,[3] because of the observed linear dependence of the pulse-height defect with fragment mass, $V_2/(V_1+V_2)$ is linearly related to $E_2/(E_1+E_2)$, where E_1 and E_2 are the kinetic energies of the pair fragments. From the conservation of momentum it follows that the output $V_2/(V_1+V_2)$ is proportional to the fragment mass M_1, if it is assumed that no neutrons were emitted from the

fragments. The procedure adopted for the calibration of $V_2/(V_1+V_2)$ versus fragment mass and the correction of the mass distribution for the effects of neutron emission and experimental mass dispersion are described in the Appendix. The output of the adder-divider circuit was fed to a 1024-channel analyzer, divided into four quarters of 256 channels each. The mass distribution without coincidence with any secondary radiation was recorded in the first quarter of the analyzer memory.

The pusle heights from the x-ray detector were calibrated into energies using the sources of Am^{241}, Co^{57}, Cs^{137}, Ba^{133}, and Gd^{153}. The full width at half-maximum (FWHM) of the Ba $K\alpha$ line was found to be about 10.0 keV. The relationship between energy resolution of the x-ray detector system and the photon energy was also experimentally obtained using the calibration sources. A high precision pulser fed at the input of the x-ray detector amplifier was also calibrated with respect to x-ray energies. The pulse heights from the x-ray detector system corresponding to the light fragment K x-ray energy group (8–21.1 keV) and the heavy fragment K x-ray energy group (21.1–50 keV) were selected with two single-channel analyzers using the calibrated pulser. The pulses from the fission detector D_2 and the x-ray detector were fed to a coincidence unit of resolution time (2τ) of 1.2 μsec to ensure 100% coincidence efficiency. The single-channel analyzer outputs were gated with the coincidence pulse to select the light and heavy fragment K x rays, respectively. These pulses selecting light and heavy fragment K x rays were used to steer the pulse-height analyzer so that if there was a pulse corresponding to the detected light fragment or heavy fragment K x ray, the $V_2/(V_1+V_2)$ output was stored in the $\frac{2}{4}$ or $\frac{3}{4}$ of the analyzer memory, respectively, instead of in the $\frac{1}{4}$ quarter. In this way, the data recorded simultaneously in the $\frac{1}{4}$, $\frac{2}{4}$,

and $\frac{3}{4}$ of the analyzer memory represented the normal fragment mass distribution, mass distribution in coincidence with light fragment K x rays, and in coincidence with heavy fragment K x rays, respectively. The K x-ray spectrum was also recorded periodically by gating the NaI(Tl) detector output with the fragment x-ray coincidence pulse.

In 15 separate runs of 24 h each about 10^5 triple coincidence events corresponding to 2.36×10^7 binary events were recorded. To ensure the stability of the selected energy windows, the energy calibration of the precision pulser and the settings of the two single-channel analyzers were checked before and after each run.

C. Background Corrections

The above measurements were carried out with and without a copper filter of thickness 440 mg/cm² to correct for the background triple coincidences. This filter was essentially opaque to the fragment K x rays (10–40 keV) and was practically transparent for the fission γ rays. The transmission of this absorber for 30- 40- and 100-keV photons was calculated to be 0.8%, 12.3, and 82.0%, respectively. The measurements taken with the absorber represented total background counts arising, first, from the true coincidences between fission and the Compton scattered fission γ rays, and, secondly, from the chance coincidences. The difference between these two measurements represented, to a good approximation, the spectra in coincidence with the K x-rays alone. A small transmission of the high-energy K x rays ($\sim$40 keV) through this filter was taken into account in correcting for the background. Measurements showed that about 40% of the total counts belonged to the background coincidences, the chance coincidences being only 15% of the total.

III. RESULTS AND ANALYSIS

The observed energy distributions of the x rays after correction for the background is shown in Fig. 3. This measurement was done earlier[10] in an experimental geometry different than that shown in Fig. 1. In this case the x-ray detector was in line with the fragment detector placed on the other side of the foil. This spectrum contains the x rays emitted from both members of the fragment pair, one moving towards and the other away from the x-ray detector; hence the Doppler shifts on the average energies is not expected. The spectrum of the x rays emitted from Cf^{252} fragments as measured by Glendenin and Griffin[1] with a NaI(Tl) detector is also shown in the figure for the sake of comparison of peak positions in the two cases.

The mass distributions $Y_X{}^L(M)$ and $Y_X{}^H(M)$ observed in coincidence with the light group and heavy

[10] R. Zaghloul, Ph.D. thesis, University of Bombay, India, 1968 (unpublished).
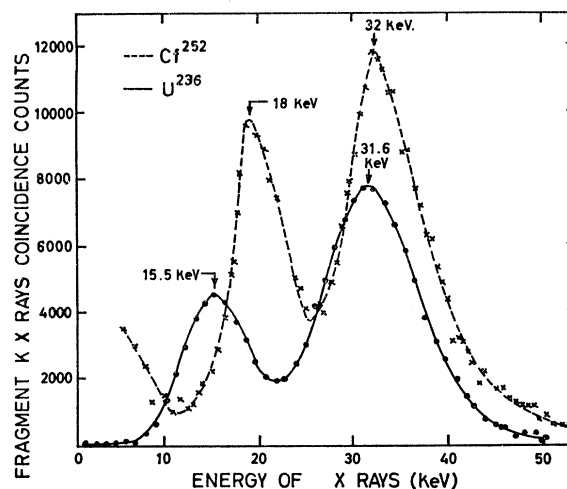
FIG. 3. Energy distribution of the K x rays after correction for background. In this measurement, the x-ray detector was placed on the other side of the foil in line with the fragment detector.

group of K x rays are shown in Fig. 4 along with the normal mass distribution $Y(M)$. Here M is the approximate preneutron emission mass, uncorrected for the effects of neutron emission and mass dispersion. The second hump in the distribution $Y_X{}^L(M)$ and the first hump in the distribution $Y_X{}^H(M)$ correspond to the cases when the light and heavy fragments, respectively, are moving towards the detector D_2. It can be seen from Fig. 1 that when the fragments are moving towards the detector D_2, the x rays emitted all along the fragment path are not seen by the x-ray detector. Therefore only the first hump in $Y_X{}^L(M)$ and the second hump in $Y_X{}^H(M)$ correspond to the unshielded view, while the other two humps correspond to a partially shielded view. The data have been analyzed separately, to obtain the observed K x-ray yield per fragment for the cases of unsheilded and partially shielded views.

The unbiased mass distribution $Y(M)$ and the distribution $Y_X(M_{L,H})$ in coincidence with the light or heavy fragment K x rays are related by

$$Y_X(M_{L,H})/Y(M) = \Omega\eta(M_{L,H})N_X(M_{L,H})$$
$$= R_X(M_{L,H}), \quad (1)$$

where $N_X(M_{L,H})$ is the average number of K x rays emitted from masses $M_{L,H}$, $\eta(M)$ is the detection efficiency for the K x rays characteristic of fragment mass M, and Ω is the solid angle of detection. Thus $R_X(M_L)$ and $R_X(M_H)$ were obtained from channel-by-channel division of the counts in the $\frac{3}{4}$ and $\frac{1}{4}$, respectively, by the counts in the $\frac{1}{4}$ of the analyzer memory. The values of $R_X(M)/\Omega$ are plotted as a function of final fragment mass M_f (after neutron emission and corrected for mass dispersion) in Fig. 5(a). The solid angle of detection Ω was calculated for the present experimental geometry with the CDC-3600 computer using a Monte Carlo method, taking into account the

finite size of the source and x-ray detector. Since the direction of fragment motion is perpendicular to the direction of x-ray detector and the x-ray detector was at a relatively large distance as compared to the foil-fragment detector distance (Fig. 1), the solid angle was calculated assuming that all the x rays were emitted at the source foil itself. This approximation can only lead to a maximum uncertainty in the calculated solid angle of about 3%, which is included in the quoted results.

A. Corrections for Energy Resolution of X-Ray Detector

The determination of $N_X(M_{L,H})$ from Eq. (1) is valid only if the pulse height selected from the single-channel window settings always correspond to the energy windows of 8–21 and 21–50 keV required for separating K x rays from the light and heavy fragment groups. However, because of a pulse-height spread in the x-ray detector output, the pulse-height distribution of the heavy-fragment x rays has a tail extending into the light-fragment x-ray window and vice versa. In addition, the escape peak of the heavy-fragment x rays of energies greater than 32 keV falls in the light-fragment x-ray region. The values of $N_X(M_{L,H})$ cor-
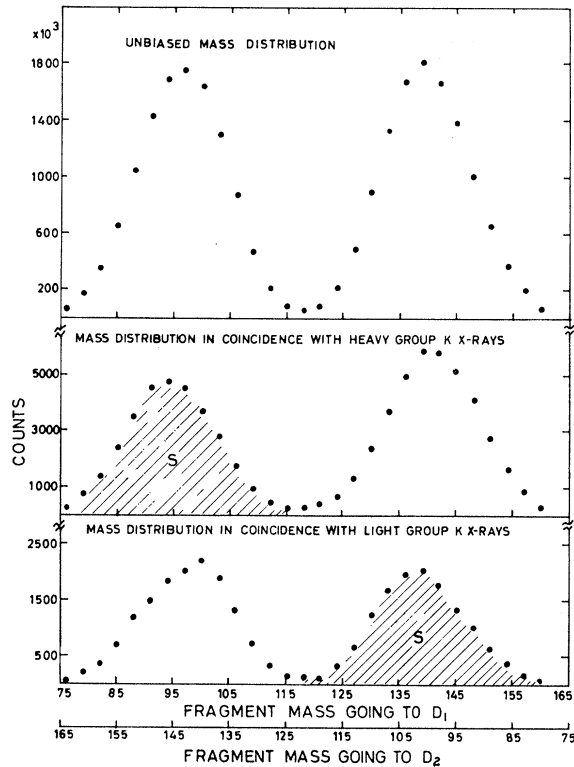
FIG. 4. Mass distributions observed in coincidence with the light and heavy group of K x rays are shown along with the observed unbiased mass distribution. The shaded humps correspond to the partially shielded view of the x-ray detector, while the other two humps are for the unshielded view.
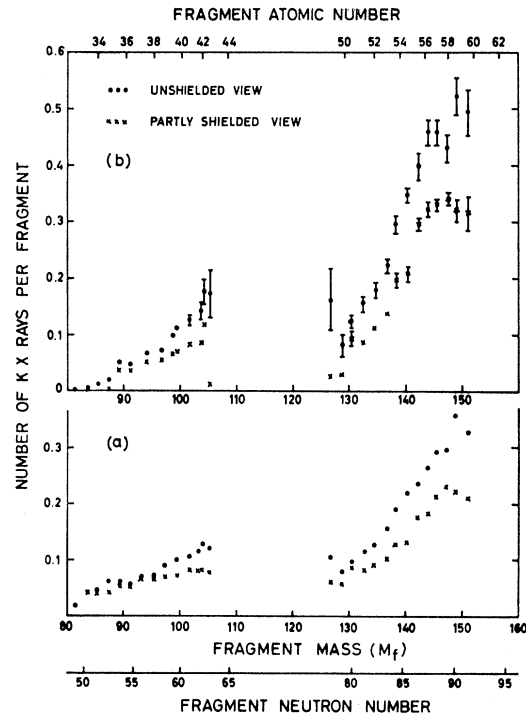
FIG. 5(a). Measured K x-ray yield uncorrected for detection efficiency and the effects of energy resolution of the x-ray detector is plotted as a function of fragment mass after neutron emission (corrected for mass dispersion shift). (b) Number of K x rays per fragment after correction for detection efficiency and the energy-resolution effects is plotted as a function of fragment mass after neutron emission (corrected for mass dispersion shift).

rected for these effects were derived in the following manner.

Let $P^R(M)$, $P^W(M)$, and $P^{\circ}(M)$ be the probabilities that an x ray emitted from mass M gets detected and gives a pulse height falling in the right window, the wrong window, and outside the window ranges, respectively. Then,

$$P^R(M) + P^W(M) + P^0(M) = \eta(M)\Omega. \qquad (2)$$

The values of $N_X(M_L)$ and $N_X(M_H)$ for a pair of complementary fragments are then related to the measured values $R_X(M_L)$ and $R_X(M_H)$ by the following equations:

$$R_X(M_L) = N_X(M_L)P^R(M_L) + N_X(M_H)P^W(M_H) \quad (3)$$

and

$$R_X(M_H) = N_X(M_H)P^R(M_H) + N_X(M_L)P^W(M_L). \quad (4)$$

The probabilities $P^R(M)$ and $P^W(M)$ were calculated using the measured response of the NaI detector for different photon energies. It was found that the experimental energy resolution (FHWM) as a function of energy E_X has the simple relation, $\mathrm{FWHM} = a\sqrt{E_X} + C$, where a and c are constants.

With this relation, Gaussian distributions of average K x-ray energies equal to those expected for emission

from different fragment masses, and having areas equal to $\eta(M)\Omega$, were computed. To calculate average K x-ray energy from fragment mass M, the corresponding fragment charge was calculated on the equal-charge-displacement hypothesis.[11] The efficiency of the 1-mm NaI crystal for different energies was calculated from the known photoelectric and total absorption cross sections, also taking into account a small attenuation of the x rays in the two beryllium windows. For x-ray energies greater than 32 keV, the resulting pulse-height distributions were taken as two separate Gaussians of average energies E and $E-28$ keV, and having areas equal to $\eta(M)\Omega[1-p(M)]$ and $\eta(M)\Omega p(M)$, respectively, where $p(M)$ is the escape probability for x rays emitted from mass M. The areas under the two Gaussians in the ranges 8–21.0 and 21.0–50 keV were computed by numerical integration to obtain the values of $P^R(M_L)$, $P^W(M_L)$, $P^R(M_H)$, and $P^W(M_H)$. The number $N_X(M)$ of K x rays per fragment obtained from Eqs. (3) and (4) are plotted against the fragment mass M_f after neutron emission in Fig. 5(b), both for the cases of unshielded and partially shielded views. The K x ray yields per fragment for different fragment masses shown in Fig. 5 have been corrected for the effects of experimental mass resolution in an average manner by plotting the yield at the mass corrected for the mass-dispersion shift. Consequently the x-ray yield for any mass M_f should be interpreted to represent a weighted average yield over a few neighboring fragment masses. The observed smooth variation of the yield with fragment mass therefore does not rule out the possibility of different K x-ray yield from neighboring odd and even masses. Nevertheless, the present results do show the average behavior of the variation of the K x-ray yield as a function of fragment mass for U^{236} fragments similar to the earlier measurements[1,2] for Cf^{252} fragments.

From the measured yield per fragment for the unshielded view, the average number of K x rays emitted from the light and heavy groups were calculated and the values are given in Table I. The results of other measurements are also shown in the table for comparison. From the present data the average number of K vacancies per fission is calculated to be 0.12+0.01 for the light group and 0.35+0.02 for the heavy group. The ratio of the observed number of K x rays for the unshielded and shielded views are found to be 1.42 ±0.09 and 1.54±0.09 for emission from the light and heavy groups, respectively. From the experimental geometry it is found that in the case of the partially shielded view, the observed yield refers to only those x rays emitted in the initial 0.9 cm of the fragment path. On this basis, the observed ratios correspond to average x-ray half-lives of 0.36±0.05 and 0.62±0.07 nsec for

[11] L. E. Glendenin, C. D. Coryell, and R. R. Edwards, in *Radiochemical Studies: The Fission Products*, edited by C. D. Coryell and N. Sugarman (McGraw-Hill Book Co., New York, 1951), P. 489.

TABLE I. Light- and heavy-fragment K x-ray yield for U^{236} fission fragments.

Light-fragment yield [(K x rays)/fission]	Heavy-fragment yield [(K x rays)/fission]	Ref.
0.08±0.01	0.30±0.02	This work
0.10±0.03	0.42±0.12	5
0.08	0.12	6
0.17±0.02	0.43±0.04	7
0.12±0.03	0.20±0.05	8
0.18±0.06	0.39±0.09	9

the light and heavy groups, respectively, assuming a single decay constant. It may be noted, however, that the assumption of a single decay constant is unrealistic. In fact a continuous spectrum of various half-life components can be expected for each fragment group firstly because of different possible γ half-lives and secondly because of different values of conversion coefficients. The half-lives estimated here therefore correspond to a suitably weighted average over the fragment group of the product of γ half-life, and the inverse of corresponding internal-conversion probability for different transitions.

IV. DISCUSSION

For the purpose of comparison, the present results on K x-ray yield from U^{236} fragments (unshielded view) are shown in Fig. 6 together with the previously[2] measured K x-ray yield from Cf^{252} fragments. Since the light peak of the mass distribution is at a lower mass in the fission of U^{236} as compared to that in the fission of Cf^{252}, in this work it has been also possible to obtain data for fragment masses less than 90 in the region of neutron closed shell of $N=50$ for which no
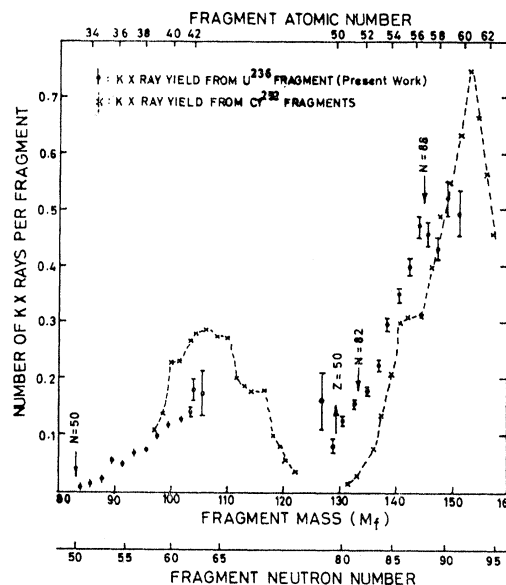

FIG. 6. Comparison of K x-ray yield from U^{236} and Cf^{252} fragments.

data were available from Cf^{252} studies. The K x-ray yield curve for Cf^{252} has been interpreted earlier[1-4] on the basis of the variation of the internal-conversion probability as a function of mass, as expected from the characteristics of the low-lying states. The present results on the yield from U^{236} fragments are consistent with the interpretations previously put forward for the case of Cf^{252}. As expected, the x-ray yield is found to be vanishingly small for fragments of mass around 84 that have a closed neutron shell of $N=50$. As one moves away from this closed shell, the yield is found to increase up to mass 106, similar to the case of emission from Cf^{252} fragments. Since both the U^{236} and the Cf^{252} fragments are neutron rich to nearly the same extent, the present results are consistent with the proposal[2-4,12] that the neutron-rich fragments around mass 106 make up a new region of deformation and therefore deexcite with lower-energy, highly converted transitions. However, an alternative explanation for the observed high K x-ray yield in this region could be that in the neutron-rich even nuclei around mass 106 the first-excited state is 0^+ leading to $0^+ \rightarrow 0^+$ transitions.

For the heavy group of U^{236} fragments, the minimum in the yield is also found to be in the region of closed $Z=50$ and $N=82$ shells, similar to the case of Cf^{252}. However, the striking increase in the yield for masses greater than 144 (corresponding to $N>88$) observed for the case of Cf^{252} does not seem to be apparent for the case of U^{236}. On the other hand, the yield from U^{236} fragments appears to be nearly constant or somewhat decreasing with increasing mass for fragment masses between 144 and 151. This effect appears to be similar to that reported earlier[1,2] for Cf^{252}, where a drop in the yield beyond mass 153 was observed, although the region of stable deformation is known to extend to mass 180. Atneoson et al.[3] have pointed out that this drop in the yield may be connected with the possibility that these fragments ($M_f>153$) are not being formed with sufficient spin to undergo a cascade of rotational transitions. It has been suggested that closed-shell spherical nuclei that cannot receive spin by simple Coulomb interaction may also be less effective in imparting spin to the partner fragment which may be deformed. Consequently, fragments of mass greater than 153 may be formed with continually decreasing spin because these fragments at scission will be paired off with fragments approaching spherical shape, due to the proximity with $N=50$ shell. It is possible to test these arguments by a comparison of the K x-ray yield for U^{236} and Cf^{252} fragments, since mass of the heavy fragment paired off with the light fragment having $N=50$ is different in the two cases. On the basis of the observed[13] number of neutrons as a function of fragment mass we assume that because of the neutron closed shell at $N=50$ the scission deformation of the

light fragment is continuously decreasing below masses 97 and 90 for the cases of Cf^{252} and U^{236} fragments, respectively. The corresponding masses of the partner heavy fragments after neutron emission are 152 and 144, in two cases. Therefore, it can be expected that the spin imparted to the heavy fragment decreases as one moves beyond these masses. The drop in the x-ray yield for the Cf^{252} fragments does indeed appear at about mass 153. For emission from U^{236} fragments also, the points in Fig. 5(b) can be interpreted either to suggest a decrease in the yield beyond mass 144 or at least a constant yield between masses 144 to 151. It therefore appears quite likely that the absence of a striking increase in the x-ray yield for masses beyond 144 (corresponding to $N=88$) for the case of U^{236} fragments is due to the pairing off of these fragments with undeformed partners having $N \sim 50$. The present results therefore favor the argument that the x-ray yield depends both on the properties of the low-lying states and the intiial spin of the fragment. Note that in some recent determination[4] of the K x-ray yield from Cf^{252} fragments as a function of fragment atomic numbers, the decrease in the K x-ray yield for $Z>60$ corresponding to $M_f >153$ is not evident. If this observation does not arise because of any uncertainities in the fragment-charge yield curve used for the above determination, one has to assume that the shapes of the K x-ray yield curve differ when plotted as a function of fragment mass and atomic number. It will be interesting to determine, with a high-resolution Li-drifted silicon detector, the K x-ray yield as a function of fragment charge for U^{236} fragments to see whether such a difference is apparent in this case also. The above arguments based on the role of initial spin of the fragments are valid only if the variation of the K x-ray yield as a function of fragment atomic number is similar to that as a function of mass number.

ACKNOWLEDGMENTS

APPENDIX: MASS CALIBRATION AND CORRECTION FOR MASS DISPERSION

The fragment masses are derived from the fragment kinetic energies with the momentum conservation relation. If E_1^* and E_2^* are the fragment kinetic energies

[12] S. A. E. Johansson, Nucl. Phys. **60**, 378 (1964).
[13] J. Terrell, Phys. Rev. **127**, 880 (1962).

before neutron emission, it follows that

$$M_1 = 236 E_2^* / (E_1^* + E_2^*).$$

The effect of neutron emission on the mass distribution arises from the following two factors: First, it introduces a dispersion in the fragment mass because of the variation in the neutron number, direction and energy. This dispersion increases[13] the variance of the mass distribution by about 2.8 (mass unit)^2. Secondly, the calculated mass M_1^c obtained from the ratio $E_2/(E_1 + E_2)$ will be shifted with respect to the actual mass depending on the number of neutrons emitted. The difference between the calculated mass M_1^c and actual mass M_1 is given by

$$M_1^c - M_1 = (M_2 \nu_1 - M_1 \nu_2)/236, \qquad (5)$$

where ν_1 and ν_2 are the number of neutron emitted by fragments 1 and 2.
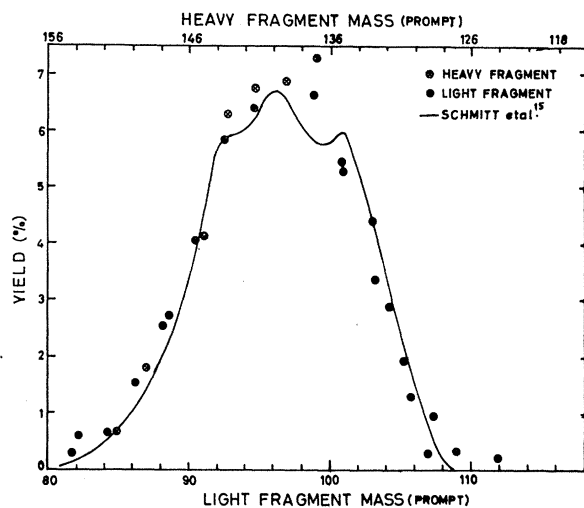

FIG. 7. Mass distribution curve obtained with the adder-divider circuit and after corrections described in the Appendix is compared with the measurements of Schmitt *et al.* (Ref. 15).

On the basis of available data the pulse height from the fragment detector varies linearly[14] with fragment energy and mass. In this case the pulse-height ratio $V_2/(V_1 + V_2)$ also varies linearly[3] with the energy ratio $E_2/(E_1 + E_2)$ and consequently distribution in the pulse-height ratio gives the distribution of the fragment mass M_1^c.

For the mass calibration, the calculated masses M_1^c for the two peaks and one minimum of the mass distribution curve were ascertained from the data of Schmitt *et al.*[15] The channel numbers corresponding to the same points in our mass-yield data were ascertained and a least-squares fit gave the relationship between calculated masses and channel number.

The mass distributions thus obtained are shown in Fig. 4, where the fragment mass refers to that uncorrected for the effects of neutron emission and mass dispersion. The variance of the observed binary mass distribution is about 65 (mass unit)^2 indicating a variance of about 15.8 (mass unit)^2 for the mass dispersion function that is attributable largely to the instrumental effects. Correction for the experimental mass dispersion shift was carried out using the method of Terrell.[13] The initial fragment masses corresponding to the new calculated masses corrected for the mass dispersion shift were obtained with Eq. (5). The experimental mass yield curve corrected for mass dispersion effects is compared with that obtained by Schmitt *et al.*[15] in Fig. 7. The observed good agreement between the two curves ensures the consistency of the procedure adopted for mass calibration and dispersion correction. The final fragment masses M_f representing the masses of fragment nuclei undergoing γ de-excitation were obtained by substracting the number of neutrons emitted from different masses.

[14] H. W. Schmitt, W. H. Gibson, J. H. Neiler, F. J. Walter, and T. D. Thomas, *Physics and Chemistry of Fission* (International Atomic Energy Agency, Vienna, 1965), Vol. 1, p. 531.

[15] H. W. Schmitt, J. H. Neiler, and F. J. Walter, Phys. Rev. **141**, 1148 (1966).